A Parametric Study on Architectures Using Common-Pressure Rail Systems and Multi-Chamber Cylinders.

Mateus Bertolin, Andrea Vacca

Purdue University/Maha Fluid Power Research Center, matbertolin@hotmail.com
Purdue University/Maha Fluid Power Research Center, avacca@purdue.edu

Abstract.

Amidst the increasing need to improve efficiency of fluid power systems in off-road vehicles, different architectures have been proposed in literature to reduce system throttling losses. Among the most cited ones, are architectures based on the use of common-pressure rails (CPRs), which in some cases have been combined with multi-chamber cylinders to further reduce power loss. This kind of solution appears to be particularly attractive in systems with several actuators with many instances of overrunning loads, such as in earthmoving machines. In this scenario, a basic question arises concerning the maximum amount of energy that can be saved by adding extra pressure rails and/or cylinder chambers. Answering this question can be challenging given that many parameters such as cylinder areas and pressure levels can affect the results for a given application. This paper proposes an extended parametric analysis that compares different architectures considering an optimized design for each solution considered. While ensuring design feasibility, the proposed algorithm finds the optimal system parameters (e.g., cylinder areas and pressure levels) for each architecture. The particular case of reference is an excavator, for which an instantaneous-optimization controller is used to ensure near-optimal control and cycle tracking for each design. Results show that even when compared to the already efficient architectures available in literature, a reduction of up to 29.3% power consumption can still be achieved with the most efficient solution. Obviously, the most suitable solution results from a compromise between implementation cost and energy efficiency. The paper qualitatively addresses these aspects.

Keywords. Common Pressure Rails, Multi-chamber cylinders, Multi-pressure rails, Off-road vehicles, Excavators.

1. INTRODUCTION

Increasing environmental awareness and governmental push towards lower carbon emissions has led the mobile machinery industry towards the development of more efficient systems. When it comes to off-road vehicles, there is an increasing trend towards the electrification of small, compact construction and agricultural machines. Nevertheless, in the case of larger and high-productivity machines, replacing the engine with an electric prime mover still imposes challenges, and many OEMs are also considering alternatives such as electric hybrids, hydraulic hybrids and hydrogen powered machines.

Regardless of the technology of choice for the prime mover, it is agreed among the technical community that the transmission efficiency of the hydraulic actuation system must increase to reduce environmental impact, machine autonomy, and operational costs.

1.1. Common Pressure Rails Systems

In the above scenario, many solutions have been proposed to improve the efficiency of fluid power systems in multi-actuators off-road vehicles, commonly aiming at reducing throttling losses. An approach that has gained interest in recent years is based on the Common Pressure Rails (CPRs) concept. In these architectures, multiple actuators share common supply lines, kept at different pressure levels. The hydraulic circuit is designed such that all actuator chambers can be connected to any of these supply lines. The concept was first introduced by Lumkes and Andruch [1]. The idea was further improved by the STEAM architecture which added accumulators to at least two of these pressure rails. Adding these accumulators opened the possibility for energy storage within the system and for advanced secondary control like strategies for the cylinders. The concept was presented by Vukovic, Sgro and Murrenhoff [2], with a prototype 18 ton. excavator being presented in [3]. This machine achieved up to 55% improvement in efficiency for an air grading cycle with a circuit that achieved the same functionality as the one showed in Figure 1.1 (a).

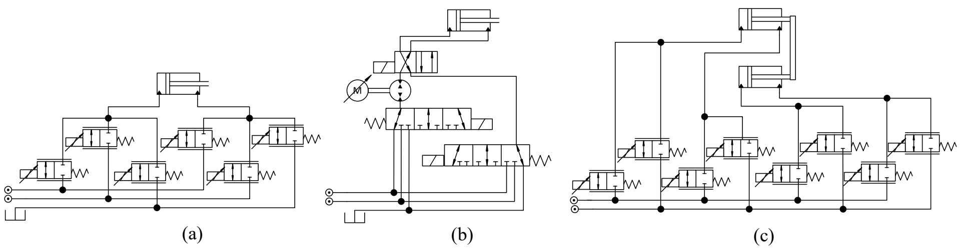

Figure 1.1. Conceptual schematics of architectures proposed byVukovic, Sgro and Murrenhoff (a), Li, Siefert and Bigelow (b) and Heybroek and Sahlman (c).

In a similar fashion, Li, Siefert and Bigelow [4] proposed an architecture with hydraulic accumulators and three pressure rails. However, in their case, it was proposed to substitute the valves - which can only waste power in throttling losses - with a pump/motor that is driving/being driven by an electric machine. This architecture is shown in Figure 1.1 (b). More recently, Guo et al [5]. proposed to use CPRs for agricultural machines, achieving an average efficiency improvement of 45%.

1.2. Multi-Chamber Cylinders and CPRs

Another approach to CPRs is based on the principle of digital hydraulics. By using linear actuators with more than 2 chambers, it is possible to increase even further the efficiency of CPRs systems. This is because the efficiency of such system increases with a larger number of achievable force levels, which is given by

$$n_{FL} = n_{PR}^{n_{CC}} \tag{1}$$

where n_{FL} is the number of available force levels, n_{PR} is the number of pressure rails and n_{CC} is the number of cylinder chambers. The idea was initially proposed by Linjama et al. [6]. Many studies have been carried out for multi-chamber cylinders, but the most successful is the implementation in a 30 ton. excavator by Heybroek and Sahlman [7] which achieved fuel efficiency gains in the range of 34-60%. This architecture is presented in Figure 1.1 (c). In a similar fashion, Dell'Amico et al. proposed using a 4-chamber cylinder with 3 pressure rails, but the architecture has only been implemented in a lab experimental set-up [8].

With respect to the design of multi-chamber cylinders, Huova and Linjama [9] showed that system efficiency can be improved by proper area selection. Nevertheless, no specific selection procedure was described. Belan et al. [10] proposed a method for designing multi-chamber cylinders in aircraft applications. In their work, the goal was to extend the number of available forces in retraction direction and a serial linkage design was used. Although no specific consideration was made with respect to the efficiency of the selected areas, the authors limited the maximum gap between force levels.

1.3. Paper Scope

Although intuition based on (1) can qualitatively give an idea of how different architectures would be ranked in terms of efficiency, to the authors' knowledge no formal analysis has been carried to quantify efficiency differences between these systems.

Admittedly, a more significant comparison would be in terms of cost-convenience for each architecture, based on parameters like return of investment time. However, such analysis still requires an estimation of the operational costs and, therefore, efficiency comparison becomes a crucial point of such analysis.

In this context, it is interesting to understand how the design of a multi-chamber cylinder, with its internal areas, affects the system efficiency. Past multi-chamber cylinder design approaches attempted keeping a constant gap between the force levels inherently realizable by the cylinder. However, it is important to understand if a different design approach for the cylinder areas could bring to further energy efficiency benefits.

As classified by Kolks and Weber [11] multi-chamber cylinders can be divided into three different arrangements: serial linkage, parallel linkage and convolution. While the series linkage design may be the simpler choice from the manufacturing point of view, the fact that it requires at least twice the length of a usual cylinder makes its application to off-road vehicles prohibitive. Parallel linkage design on the other hand results in bulkier solutions. For these reasons, industry and academia have shifted their attention mostly towards the convolution design, especially for off-road vehicle applications. A conceptual drawing of this design is shown in Figure 1.2.

The proposed study focuses on cylinders with at most 4 chambers. This is because previous works do not show practical implementations for cylinders with larger number of chambers. In addition, architectures with at most 3 pressure rails are analyzed. Intuitively, the higher is the number of rails the more is the potential for energy saving. Nonetheless, the cost is higher. A study performed by Guo et. al [5] shows that the efficiency gains per pressure rail added significantly decrease after 3 rails. Despite that work considered a different application, also this work limits the analysis to 3 rails. Nonetheless, the methodology proposed here could also be extended to architectures with a larger number of rails.

Taking a convolution design as the arrangement of choice, this paper undertakes a full factorial search to find the optimal cylinder areas, given different levels of pressure in the supply lines. The cylinder control method and the effect of the controller gain in the energy efficiency are also briefly discussed. The result is a step-by-step cylinder design procedure that maximizes efficiency for a given duty cycle. The paper will also perform a comparison between optimal solutions for different architectures.

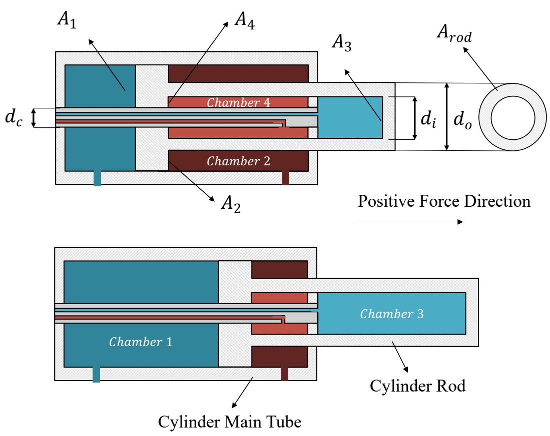

Figure 1.2. Convolution Design Conceptual Drawing

The paper structure is as follows: first, the reference machine and duty cycle are introduced in section 2. Then, a parametrization procedure is discussed, and the design constraints of the convolution arrangement are analyzed (section 3). Section 4 considers the effects of the valves actual size and the variability of the rails pressure levels. Then, a supervisory controller for managing the local cylinder control is described, followed by a description of the cylinder area optimization approach. Next, area optimization results for the arm cylinder of the reference machine are presented, followed by a comparison with other established design methods. An architecture comparison that includes all the actuators of the reference machine is discussed in section 9. Lastly, the main conclusions of this work are discussed and summarized.

2. Reference Machine and Duty Cycle

This work takes as reference machine a 20 ton. excavator. Considering that the energy efficiency of off-road machines is heavily dependent on the specific duty-cycle, this paper proposes a cycle-dependent optimization. It takes as reference a 90° truck loading cycle, which is typically used to evaluate the efficiency of excavators. Examples include [7] and

[12]. In these working conditions, the machine digs into the ground, rotates 90° while lifting the boom actuator. It then dumps the bucket content into a truck with the boom fully extended. Real-world data coming from expert operator measurements were available to the authors and were used as input to the proposed optimization algorithm. The data included measured actuator pressures as well as cylinder positions.

3. Multi-Chamber Cylinder Design Parametrization and Design Space Generation

The following paragraphs formalize the space domain of the feasible multi-chamber cylinder designs that can be suitable for a given application. In this analysis, it is assumed that the required maximum and minimum forces are previously known based on the baseline machine specifications. The system design starts with a selection of the minimum pressure allowed in the rail with the highest pressure, as well as the maximum pressure allowed in the pressure rail with the lowest pressure level. This is done to ensure maximum force availability, regardless of the pressure levels in the rails, which can vary over time despite the large capacitance added by accumulators. Then, the total areas in the positive and negative directions are obtained by solving the following system of equations

$$\begin{aligned} p_{HP,min}\, A_{pos} - p_{LP,max} A_{neg} &= F_{max} \\ p_{LP,max}\, A_{pos} - p_{HP,min} A_{neg} &= F_{min} \end{aligned} \tag{2}$$

where A_{pos} is the total area in the positive direction and A_{neg} is the total area in the negative direction. Considering a general case, it is possible to define

$$\begin{aligned} A_{pos} &= A_1 + A_3 + A_5 + \cdots + A_{2n-1} \\ A_{neg} &= A_2 + A_4 + A_6 + \cdots + A_{2m} \end{aligned} \tag{3}$$

where n is the total number of chambers acting in the positive direction, and m is the total number of chambers acting in the negative direction. The cylinder design can then be parametrized by $P = (n + m - 2)$ parameters given by

$$\begin{aligned} r_{2i-1} &= A_{2i+1}/A_1, \ i = 1,2, \dots, n \\ r_{2j} &= A_{2j+2}/A_2, \ \ j = 1,2, \dots, m \end{aligned} \tag{4}$$

Considering the case of a cylinder with at most 2 chambers acting in each direction:

$$A_{pos} = A_1 + A_3 = A_1(1 + r_1), \quad r_1 = A_3/A_1$$
$$A_{neg} = A_2 + A_4 = A_2(1 + r_2), \quad r_2 = A_4/A_2 \tag{5}$$

In this way, the number of design parameters is reduced to only two: r_1, the ratio of areas in the positive direction and r_2 the ratio of areas in the negative direction. Note that, even though the case of a 4-chamber cylinder is considered, cylinders with 2 and 3 chambers can be considered in this analysis by making r_1 and/or r_2 = 0.

To establish a clear relationship between the parameters r_1 and r_2 and the actual cylinder design specifications, a few diameters are defined according to Figure 1.2. They are the cylinder central diameter (d_c), the rod inner diameter (d_i), and the rod outer diameter (d_o). By inspection of the geometry, the following design constraints can be derived:

A. $A_1 = A_2 + A_4 + A_{rod}$
B. $A_{1,min} = \frac{\pi}{4}(d_o^2 - d_i^2)$
C. $A_{3,min} = \frac{\pi}{4} \cdot d_c^2$
D. $A_4 = \frac{\pi}{4}(d_i^2 - d_c^2) = \frac{\pi}{4}\left(\frac{4}{\pi} \cdot \frac{A_{pos}}{(1+r_1)} \cdot r_1 - d_c^2\right)$

With the constraints A-D defined, the cylinder rod area can be obtained by

$$A_{rod} = \frac{\pi}{4}(d_0^2 - d_i^2) \tag{6}$$

In addition,

$$A_3 = \frac{\pi}{4} \cdot d_i^2 \tag{7}$$

Manipulating (6) and (7) and substituting in the physical constraint A, it is possible to show that

$$d_o = \sqrt{(A_{pos} - A_{neg})\, 4/\pi} \tag{8}$$

3.1. Inner Rod Diameter Minimum Value

Although other solutions are possible, this work considers that the hydraulic connection to chambers 3 and 4 is done through an inner connection inside the main cylinder tube. This means that, in practice, it is necessary to ensure that there is enough space for the hydraulic connection. Therefore, a fifth constraint is obtained

E. $d_{c,min} \leq d_c \leq d_i$

It is worth mentioning that this requirement for a minimum central diameter also imposes a constraint on the minimum value of the rod inner diameter (d_i). Consequently, it also imposes a constraint on the minimum value of A_3, as highlighted by constraint C and E.

3.2. Buckling Analysis and r_1 Maximum Value

The design space should exclude the cylinders that do not satisfy the Euler's critical load for buckling. It is worth mentioning that for the proposed design, only the load bared by chamber one can cause the rod buckling. Therefore,

$$F_{max,buck} = p_{HP,max} \cdot A_1 = p_{HP,max} \cdot \frac{A_{pos}}{1+r_1} \tag{9}$$

The cylinder safety coefficient is then defined as

$$S_c = \frac{F_{cri}}{F_{max,buck}}, \qquad F_{cri} = \frac{\pi^2 E\, I_{min}}{(KL)^2}, \qquad I_{min} = \frac{\pi}{64}(d_o^4 - d_i^4) \tag{10}$$

By re-writing (10) in terms of A_{pos}, A_{neg} and r_1, it can be shown that there is a direct relationship between the safety factor and the parameter r_1. This is shown in Figure 3.1, which points out that there is a limit to the maximum value of r_1 ($r_{1,max}$). This ultimately leads to a limitation on the maximum value of A_3, and, based on (7), to the maximum value of the rod inner diameter (d_i). Therefore, a sixth constraint is added:

F. $d_c \leq d_i \leq d_{i,max}$

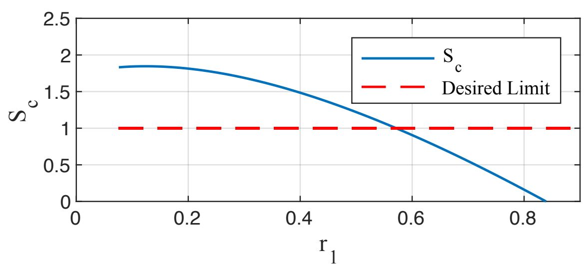

Figure 3.1. Normalized S_c vs r_1 for one of the actuators of the reference machine.

3.3. Cylinder Design Space

With all the constraints determined, the complete design space can be generated. Different designs are created by varying the diameters d_i and d_c, within pre-determined ranges obtained with constraints E and F. The design space generation procedure is summarized as follows:

1. Define $p_{HP,min}$ and $p_{LP,max}$.
2. Solve (2) to determine A_{pos} and A_{neg} given F_{max} and F_{min}.
3. Evaluate d_o with (8).
4. Define $d_{c,min}$ and evaluate $r_{1,min}$.
5. Discretize r_1 within the range $r_{1,min} \leq r_1 \leq 1$. Evaluate S_c for each r_1 and determine $r_{1,max}$ based on buckling analysis.
6. Re-discretize r_1 within the range $r_{1,min} \leq r_1 \leq r_{1,max}$. For each value of r_1, determine d_i.
7. For each value of r_1, discretize values of d_c within the range $d_{c,min} \leq d_c \leq d_i$.

Because of the physical constraint D, there is a clear relationship between r_1 and A_4. Consequently, there is also a relationship between r_1 and the achievable r_2. By manipulating the definition in eq. (5), and using constraints D and E, it can be shown that the feasible range of r_2 will be limited with this limitation being a function of r_1. In this way, once $r_{1,min}$ and $r_{1,max}$ are defined, a feasible range for r_2 can be found for each value of r_1. Such result is clearly seen in the final design space presented in Figure 3.2.

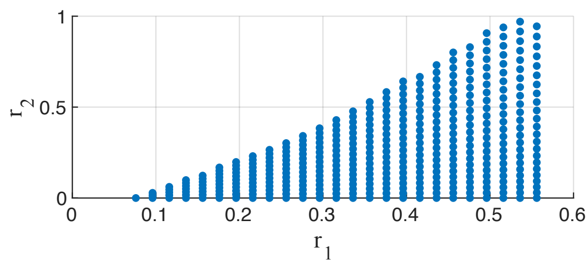

Figure 3.2. Final feasible design space for the boom cylinder of the reference machine.

4. Considerations on Valve Size and Medium Pressure Rail Level

Considering that the focus of the proposed optimization is to improve efficiency, two important factors beyond the cylinder design can impact the results. They are valve size and medium pressure level (in architectures with 3 pressure rails). With respect to the first one, this study assumes that each valve is sized for a user defined maximum pressure drop (Δp_v) at its maximum flowrate. Since different chambers will have different maximum flowrates, this means that valves are sized accordingly to the chamber they are connected to.

Another relevant factor is the pressure level used in the medium pressure rail, p_{MP}. Intuitively, the average between maximum and minimum pressure can be a good choice. However, this work evaluates each cylinder design considering different possibilities for the p_{MP} value. This is done by adding a third variable parameter to define the overall design architecture. Besides varying r_1 and r_2, which define the cylinder areas, a third parameter r_3 defines the pressure in the intermediate pressure level according to

$$p_{MP} = (p_{HP} - p_{LP}) \cdot r_3 + p_{LP}, \qquad 0 \leq r_3 \leq 0.9 \tag{11}$$

In the proposed analysis, supply pressures are assumed constant. It is important to observe that the case of systems with two pressure rails are included in the analysis. In fact, in Eq. (11) when $r_3 = 0$, p_{MP} becomes equal to p_{LP}, which corresponds to the case of a system with 2 pressure rails.

5. CYLINDER CONTROL

One of the main advantages of architectures using CPRs and multi-chamber cylinders is the opportunity to configure the cylinder connections to the pressure rails so that throttling losses are reduced. This means that, for an efficient operation, each actuator requires a supervisory controller that selects the best connections between different rails and chambers based on the current cylinder load.

This work uses an approach similar to the Force Index Controller (FIC) proposed by Sjoberg and Heybroek [13], but with modifications in the cost evaluation as expressed by the cost function (12), (13) and (14). In this way, all terms in the cost function have energy units. The instantaneous optimization controller selects the configuration id that minimizes the losses in the cylinder at the time step k according to

$$J_{k,k-1}(id) = E_{th,k}(id) + W_{sw} \cdot E_{sw,k,k-1}(id) \tag{12}$$

where the first term evaluates the throttling losses

$$E_{th,k}(id) = \left|\dot{x}_{meas,k} \cdot t_s \cdot \left[F_{meas,k} - F(id)\right]\right| \tag{13}$$

and the second term accounts for the compressibility losses, according to

$$E_{sw,k,k-1}(id) = \sum_{i=1}^{4} \frac{V_{i,k}}{B} p_{i,k}(id) \cdot (p_{i,k}(id) - p_{i,k-1}) \tag{14}$$

where $V_{i,k}$ is instantaneous volume of chamber i, at time step k. More information on the derivation of eq. (14) can be found in [14]. The gain W_{sw} was proposed in [13] and is used to give more or less importance to the switching losses. Its impact on cylinder efficiency is discussed in the results section. The reference force $F_{meas,k}$ in this work is a simulation input obtained from the measured actuator pressures in the reference machine.

6. PROPOSED AREA OPTIMIZATION METHOD

A full factorial analysis of the design space (variations of the parameters r_1, r_2 and r_3) is performed to obtain a thorough comparison between different cylinder designs and system architectures. To reduce the impact of the controller switching gain W_{sw} in the results, a fourth parameter is added to the analysis

$$W_{sw} = r_4, \quad 0 \leq r_4 \leq 2 \tag{15}$$

The duty cycle measured data for a reference actuator is fed into a cylinder control block, which determines the optimal configuration for the cylinder connections between rails at that given time step. A simplified schematic is shown in Figure 6.1.

Once these connections are found, both throttling and switching losses are evaluated at the given time-step. The total losses for each design over the reference duty cycle are obtained by summing up the throttling and the compressibility losses of each time-step:

$$J_{cyl} = \sum_{k=1}^{N} E_{th,k}(id_k^*) + E_{sw,k,k-1}(id_k^*) \tag{16}$$

It is important to remark some of the key assumptions of the proposed method. First, the rails pressures are assumed constant and the valve opening dynamics are neglected. Consequently, any possible cross-leakage between rails during chamber pressure level transitions are not considered.

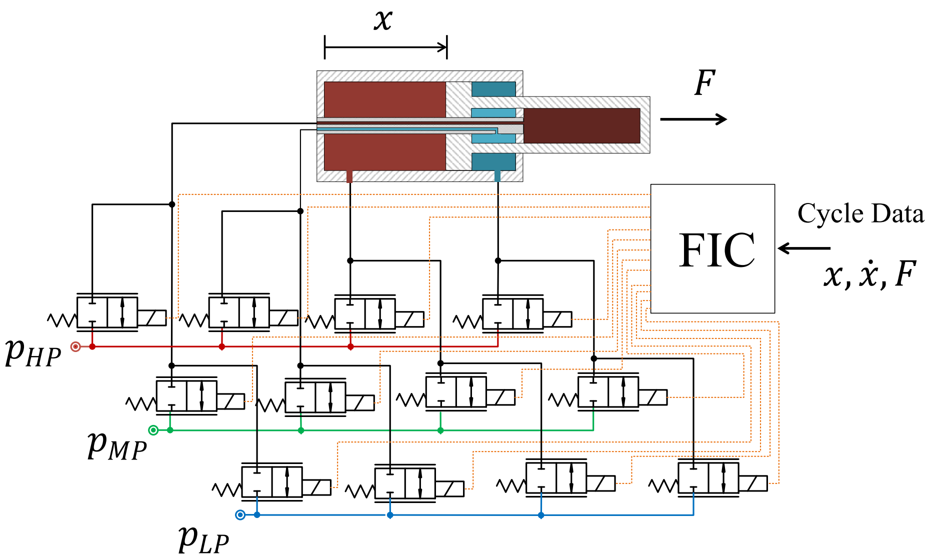

Figure 6.1. Conceptual schematic of control and hydraulic system considering the most general case in this study, with 3 pressure rails and a 4-chamber cylinder.

7. AREA OPTIMIZATION RESULTS

This section presents the area optimization results for the arm cylinder of the reference machine. Section 9 will summarize the results considering all the machine actuators. The main parameters used in the optimization are presented in Table 7.1.

Table 7.1: Main Optimization Parameters

Parameter	***Values***
$p_{HP} = p_{HP,min}$	330 bar
$p_{LP} = p_{LP,max}$	30 bar
$r_{1,arm}$	[0.076:0.02:0.576]
d_c	$[d_{c,min}: 0.002: d_{c,max}(r_1)]$
$d_{c,min}$	40 mm
r_3	[0 0.25 0.5 0.6 0.7 0.8 0.9]
r_4	[0:0.1:1.2 1.5 2]
p_{MP}	[30 105 180 210 240 270 300] bar
t_s	0.1 s
B	$1.5 \cdot 10^9$ Pa
Δp_v	10 bar

7.1. Four-Chamber Cylinders

Figure 7.1 shows the results for the entire design space (combinations of r_1 and r_2) at different levels of medium pressure rail (r_3) pressure. In each case, only the results with the most efficient controller gain ($r_4 = W_{sw}$) are shown.

First, it is clear from the comparison of the colors in Figure 7.1 (a) and (b) that losses can be considerably reduced when a third rail is added to the circuit ($r_3 \neq 0$). Although this was expected, the plot quantifies this difference reduction to be as significant as 69% when comparing systems with 81 (4 chambers and 3 rails) and 16 (4 chambers and 2 rails) force levels. In practice, this value may be lower due to cross-leakage losses during switching and due to dynamic challenges imposed by frequent switching. Nevertheless, it represents a significant margin for improvement.

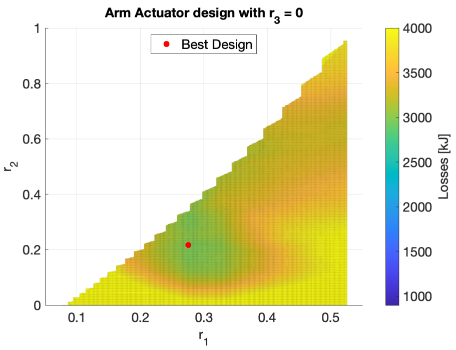

(a)

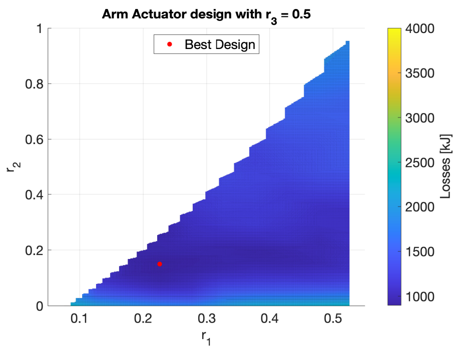

(b)

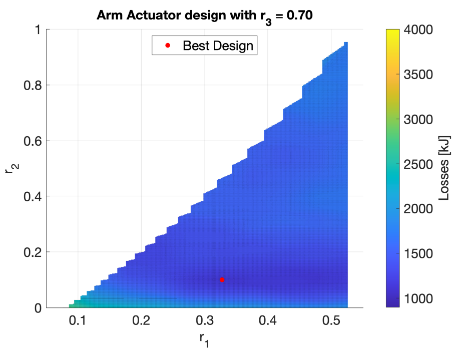

(c)

Figure 7.1. Area optimization results considering arm cylinder of reference machine with $r_3 = 0$ (a), $r_3 = 0.5$ (b) and $r_3 = 0.7$ (c).

It is also interesting to comment on the optimal areas found in each case. When only two pressure rails are used, the optimal areas differ from the typical multi-chamber cylinder design approach seen in literature [6], [7] which uses ($r_1 = r_2 = 0.25$). The rationale for such is twofold: first, this optimization is cycle dependent and therefore a finer discretization in certain operating areas may be beneficial, while the typical design approach simply achieves an even force distribution. In addition, this approach accounts for compressibility losses, which are not considered in the typical design.

When a third pressure rail is added, the optimal areas are dependent on the pressure level selected for the medium rail. This is clear by comparing the plots (b) and (c) in Figure 7.1 which show that for a higher pressure level in the medium rail, different values of r_1 and r_2 are recommended. Nonetheless, different cylinder designs can achieve a similar level of efficiency, as it is clear from Figure 7.1(b), which allows the designer to select the parameters r_1 and r_2 based on other requirements such as safety factor.

A summary of the optimal area ratios and controller gain for each value of r_3 is shown in Table 7.2. These results confirm that the medium pressure level should be placed at the average value between high and low pressure levels. Even a small difference of 30 bar in this pressure level, can lead to an increase of more than 10% in losses when compared to the optimal solution. In addition, it is noticed that both optimal r_1 and r_2 values are always below 0.44, with r_1 always being below 0.38. This is important since higher safety factors are obtained with lower values of r_1.

Another interesting observation is that the optimal controller gain W_{sw} is always less than one. This means that the switching losses have less importance in the cost function (12) when compared to the throttling losses. Nonetheless, none of the optimal solutions resulted in $r_4 = 0$. Therefore, switching losses may have lower importance when compared to the throttling losses, but optimizing the cylinder operation only for throttling losses will lead to suboptimal results.

Table 7.2. Main Optimization Results: 4-chamber Cylinder Case

r_1	r_2	r_3	W_{sw}	p_{MP} (bar)	J_{cyl} (kJ)
0.296	0.173	0	0.2	-	2,935
0.356	0.434	0.25	0.3	105	1,035
0.216	**0.147**	**0.5**	**0.2**	**180**	**896**
0.216	0.126	0.6	0.3	210	1,008
0.336	0.102	0.7	0.2	240	1,137
0.376	0.079	0.8	0.3	270	1,367
0.296	0.173	0.9	0.3	300	1,754

This can be explained by the fact that a true instantaneous optimization of the losses ($r_4 = w_{sw} = 1$) does not guarantee globally optimal control decisions. This is because (14) shows that any decision made at time step k-1, will affect the decision in the following time step. Therefore, values too high of r_4 may prevent a switch, that will occur in the near future anyways, increasing the throttling losses in the current time step. Nevertheless, it is true that cross-leakage between rails during force level switch is neglected in this analysis, while in practice slow valve dynamics can lead to a higher importance of switching losses.

7.2. Three-Chamber Cylinders

This section discusses the special case of cylinders with 3-chambers ($r_2 = 0$). A summary of the optimal solutions found for each pressure level is shown in Table 7.3. As in the case of the 4-chamber cylinders, the optimal solution is found with $r_3 = 0.5$.

When compared to the results of the more general case shown in Figure 7.1, the losses of this configuration fall somewhere between the levels of Figure 7.1(a) and Figure 7.1(b). As shown in Table 7.3, the optimal solution considering the three-chamber cylinder case has losses of 1739 kJ, which is 94% higher when compared to a system with 4-chambers and 3 rails, but 41% lower when compared to a system with 4-chambers and only 2 rails.

Table 7.3. Main Optimization Results: 3-chamber Cylinder Case

r_1	r_3	W_{sw}	p_{MP} (bar)	J_{cyl} (kJ)
0.296	0	0.2	-	4,190
0.456	0.25	0.2	105	1,907
0.256	**0.5**	**0.3**	**180**	**1,739**
0.216	0.6	0.3	210	1,860
0.476	0.7	0.2	240	1,835
0.396	0.8	0.2	270	1,923
0.336	0.9	0.2	300	2,555

Figure 7.2 (left) shows the losses for different combinations of W_{sw} and r_1 considering optimal medium pressure level, r_3 for each case. It is seen that neglecting compressibility losses ($r_4 = W_{sw} = 0$) can significantly increase losses. This figure also confirms that values of W_{sw} around 0.3 lead to a minimum in cylinder losses. With respect to the cylinder design parameter r_1, a global minimum exists around 0.25, although similar efficiency levels can be also found with larger r_1 values around 0.47.

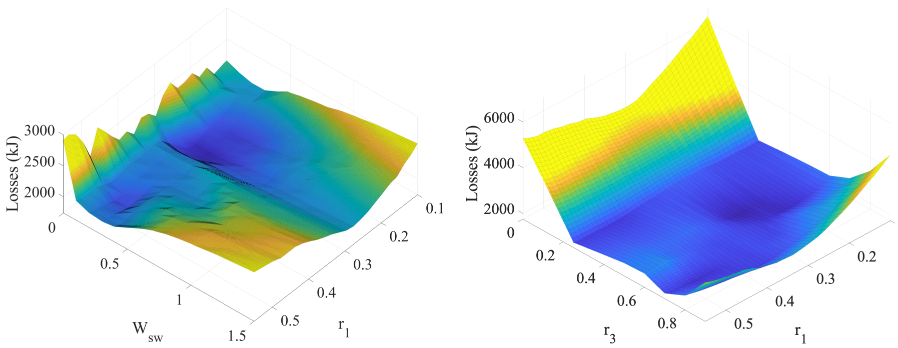

Figure 7.2. Losses as function of r_1 and W_{sw}, considering optimal r_3 and $r_2 = 0$ (left). Losses as function of r_1 and r_3, considering optimal W_{sw} and $r_2 = 0$ (rigth).

Figure 7.2 (right) shows the cylinder losses for each combination of r_1 and r_3, considering optimal controller gain selection. It is evident that there is a significant increase in losses as the value of r_3 approaches zero. In addition, a relatively small difference in losses for values of r_3 between 0.4 and 0.6 is observed, especially near the optimal cylinder design parameter ($r_1 \approx 0.25$). This means that when sizing the accumulator for the medium pressure line, a pressure variation between 150 and 210 bar can be allowed without significant increase in cylinder losses. The figure also shows that not all designs benefit from the medium pressure level at the average of the highest and lowest pressure. For example, at larger values of r_1, the system may benefit from a higher pressure in the medium pressure rail.

7.3. Two-Chamber Cylinder

To complete the analysis, a study was run forcing $r_1 = r_2 = 0$ corresponding to a 2-chamber cylinders. The results are shown in Figure 7.3. It can be seen that a minimum in losses exist at $r_3 \approx 0.25$, which differs from the cases with multi-chamber cylinders.

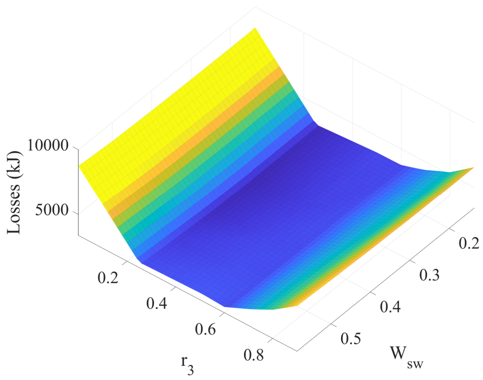

Figure 7.3. Cylinder losses for combinations of r_3 and W_{sw}, with $r_1 = r_2 = 0$

8. COMPARISON WITH ESTABLISHED DESIGN METHOD

Past work such as [6] and [8] have designed multi-chamber cylinders with an even force distribution. This means that the steps between force levels are equal. The main drawback of this solution is that it requires a given ratio α between maximum forces in the retraction and extension directions. For example, systems designed with 2 pressure rails should have the areas following the ratio 8:4:2:1, which means

$$r_1 = r_2 = 0.25, \qquad \alpha = A_{neg}/A_{pos} = 0.5 \tag{17}$$

The proposed cylinder design method, on the other hand, finds the optimal ratios r_1 and r_2 assuming that α is defined by the cylinder application[1].

Although the force ratios are different in each case, it can be interesting to discuss the force discretization obtained with the proposed optimization results with that of the established design method in literature. This comparison is shown in Figure 8.1 for the case of cylinders with 4 chambers and 2 pressure rails. The optimal solution obtained with the proposed procedure converges to a final design that achieves a force distribution very close to that of the traditional design, despite having a different force ratio, α. The drawback of setting $\alpha \neq 0.5$ is that two force levels end up being almost equal, as highlighted in Figure 8.1

However, results are different if 3 pressure rails are considered. In this case, to achieve an even force distribution the area ratios should be modified to 27:9:3:1, which results in

$$r_1 = r_2 = 0.11, \qquad \alpha = 0.33 \tag{18}$$

Additionally, the medium pressure rail level should be placed in the average of the two extreme rails. Therefore, $r_3 = 0.5$. In this scenario, the total force availability in one direction is much greater than the other, which may not be practical for some applications since it would require increasing the actuator size. This is shown in Figure 8.2.

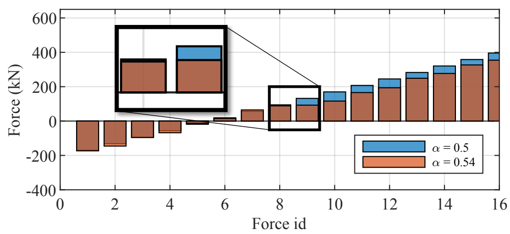

Figure 8.1. Force discretization comparison with established design method for the case of two pressure rails. Note two almost identical force levels in the design w/ α = 0.54.

Although one could argue that it is possible to adjust the force levels by reducing the highest pressure level in the system, that can be a challenging task in highly dynamic applications such as excavators that use large accumulators in their supply line. Should the maximum retraction force be needed, a large flow supply would be required to quickly increase the pressure level in a line with a large capacitance. Considering these, the optimized design results in a force discretization much more appropriate to the given application, with smaller gaps between force levels in most cases and all 81 force levels within a usable range with high pressure in one of the supply lines.

[1]It is worth noticing that it is possible to include the area ratio α in the proposed optimization procedure by solving (2) for different force ratios and repeating the optimization process for discrete values of α.

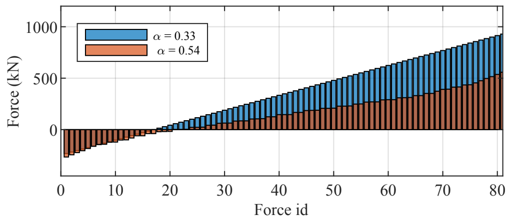

Figure 8.2. Force discretization comparison with established design for the case of three pressure rails

9. Overall System Architecture Comparison

The previous section considered only the arm cylinder of the reference machine. Obviously, the medium pressure rail level should not be optimized considering only a single actuator, since it can negatively impact the efficiency of the others. To have a better picture of the efficiency of each architecture, the following procedure was used: the total energy consumption, e.g., useful energy plus losses, was evaluated considering the optimal cylinder designs for Boom, Arm and Bucket for each discrete value of p_{MP}. The process is repeated forcing $r_2 = 0$ (3-chamber cylinders case) and forcing both $r_1 = r_2 = 0$ (2-chamber cylinder case).

Table 9.1 presents the percent difference in energy consumption between different architectures taking the system with 2-cylinder chambers and 3 pressure rails as baseline (like the STEAM system [3]). These results show that keeping the medium pressure level at the average between high and low levels is the best alternative, regardless of the number of cylinder chambers used. It also demonstrates that by adding two extra chambers to cylinders in a system with 3 pressure rails, it is possible to reduce the losses of the linear actuators by 72.4%, resulting in energy consumption reduction of 29.3%.

Table 9.1. Architecture Comparison. Energy Consumption Percent Difference when compared to baseline system.

		# Cylinder Chambers		
r_3	p_{MP} ***(bar)***	**2**	**3**	**4**
0	-	+57.6%	+ 9.9%	-8.0%
0.25	105	+5.7%	-18.9%	-28.1%
0.5	180	**baseline**	**-21.5%**	**-29.3%**
0.6	210	+3.9%	-19.5%	-28.1%
0.7	240	+5.1 %	-18.6%	-26.5%
0.8	270	+14.8%	-16.5%	-24.3%

On the other hand, results also show that efficiency gains are not as significant when adding extra chambers to the cylinders when compared to the addition of extra pressure rails.

Considering the best medium pressure level, the energy consumption reduction with respect to the baseline is of 21.5% when adding a third chamber, and 29.3% when adding a fourth.

10. CONCLUSIONS

This paper proposed a parametrization method for multi-chamber cylinders as well as a procedure to find the optimal design parameters for a given machine and duty cycle. The advantage of such approach with respect to previous works is that it allows the designer to freely select the area ratio α, and optimizes the remaining cylinder parameters. This allows for a more compact design, which can be used in wider range of applications.

The intuitive idea that adding pressure rails and cylinder chambers improves efficiency was confirmed. Nonetheless, this work quantifies that difference by showing that a reduction of up to 29.3% in cylinder power consumption is possible when comparing systems that use cylinders with 2 (baseline) and 4 chambers. In general, efficiency gains are higher when adding an extra pressure rail when compared to adding an extra cylinder chamber. It is worth mentioning that different architecture configurations will require a different number of components, e.g., valves and accumulators. Ultimately, what will lead to the success of one or another configuration is its cost-effectiveness. Although a cost evaluation is out of the scope of this work, the proposed method should provide interested companies with a clear map of how much each concept can achieve in terms of efficiency.

11. REFERENCES

[1] J. H. Lumkes Jr. and J. Andruch III, "Hydraulic Circuit for Reconfigurable and Efficient Fluid Power Systems," presented at The Twelfth Scandinavian International Conference on Fluid Power, Tampere, Finland, May, 18-20, 2011.

[2] M. Vukovic, S. Sgro, and H. Murrenhoff, "Steam - A mobile hydraulic system with engine integration," presented at The ASME/BATH 2013 Symposium on Fluid Power and Motion Control, Sarasota, Fl, Oct. 6-9, 2013, FPMC2013-4408, 2013.

[3] M. Vukovic, R. Leifeld, and H. Murrenhoff, "STEAM – a hydraulic hybrid architecture for excavators," Proceedings of the 10th International Fluid Power Conference, pp. 151–162, 2016.

[4] P. Y. Li, J. Siefert, and D. Bigelow, "A Hybrid Hydraulic-Electric Architecture (HHEA) for High Power Off-Road Mobile Machines," presented at the ASME/BATH 2019 Symposium on Fluid Power and Motion Control, Longboat Key, FL, Oct. 7-9,2019, FPMC2019-1628, 2019.

[5] X. Guo, R. Madau, J. Lengacher, A. Vacca, and R. Cardoso, "Multi-Pressure Rail System Design with Variable Pressure Control Strategy," presented at the 13th International Fluid Power Conference, Aachen, Germany, June 13-15, 2022.

[6] M. Linjama, H.-P. Vihtanen, A. Sipola, and M. Vilenius, "Secondary Controlled Multi-Chamber Hydraulic Cylinder," presented at The 11th Scandinavian

International Conference on Fluid Power SICFP'09, Linköping, Sweden, June 2-4, 2009.

[7] K. Heybroek and M. Sahlman, "A hydraulic hybrid excavator based on multi-chamber cylinders and secondary control – design and experimental validation," *International Journal of Fluid Power*, vol. 19, no. 2, pp. 1–15, 2018.

[8] A. Dell'Amico, M. Carlsson, E. Norlin, and M. Sethson, "Investigation of a Digital Hydraulic Actuation System on an Excavator Arm," in *Proceedings from the 13th Scandinavian International Conference on Fluid Power*, Linköping, Sweden, June 3-5, 2013, vol. 92, pp. 505–511, 2013, doi: 10.3384/ecp1392a50.

[9] M. Huova, A. Laamanen, and M. Linjama, "Energy efficiency of three-chamber cylinder with digital valve system," *International Journal of Fluid Power*, vol. 11, no. 3, pp. 15–22, 2010, doi: 10.1080/14399776.2010.10781011.

[10] H. C. Belan, C. C. Locateli, B. Lantto, K. Petter, and V. J. de Negri, "Digital Secondary Control Architecture for Aircraft Application," in *The Seventh Workshop on Digital Fluid Power*,Linz, Austria, Feb. 26-27,2015, pp. 21–39.

[11] G. Kolks and J. Weber, "Symmetric single rod cylinders with variable piston area? A comprehensive approach to the right solution," presented at the BATH/ASME 2018 Symposium on Fluid Power and Motion Control, Bath, UK, Sept. 12-14, 2018, doi: 10.1115/FPMC2018-8810.

[12] J. Zimmerman, E. Busquets, and M. Ivantysynova, "40% Fuel Savings By Displacement Control Leads To Lower Working Temperatures - a Simulation Study and Measurements," presented at The 52nd National Conference on Fluid Power, Las Vegas, NV, USA, 2011.

[13] K. Heybroek and J. Sjoberg, "Model Predictive Control of a Hydraulic Multichamber Actuator: A Feasibility Study," *IEEE/ASME Transactions on Mechatronics*, vol. 23, no. 3, pp. 1393–1403, 2018, doi: 10.1109/TMECH.2018.2823695.

[14] R. H. Hansen, T. O. Andersen, and H. C. Perdersen, "Analysis of discrete pressure level systems for Wave Energy Converters," in *Proceedings of 2011 International Conference on Fluid Power and Mechatronics*, 2011, pp. 552–558. doi: 10.1109/FPM.2011.6045825.

Biographies

Mateus Bertolin received his bachelor's degree in mechanical engineering from Federal University of Santa Catarina (Brazil), and the Doctorate degree in Engineering from Purdue University (USA) in 2023. Main areas of interest include optimization methods, hybrid vehicles, fluid power systems design and controls.

Andrea Vacca is a fellow of the American Society of Mechanical Engineers (ASME) and he received his Master's degree in Mechanical Engineering from the University of Parma (Italy) and his Doctoral degree in Energy Systems from the University of Florence (Italy). Currently is the director of the Maha Fluid Power Research Center, the largest academic research center dedicated to fluid power research in the United States. His research focuses on several aspects of hydraulic control technology including new concepts to perform hydraulic actuations, new designs and modeling of positive displacement machines, electrification of fluid power systems, modeling of the properties of hydraulic fluids, reduction of noise emissions from hydraulic components. His research has been funded by the U.S. Department of Energy, the U.S. Department of Agriculture, the National Science Foundation, and several industry partners